

Settling Time Optimization of a Critically Damped System with Input Shaping for Vibration Suppression Control

Minh-Duc Duong

School of Electrical and Electronic Engineering
Hanoi University of Science and Technology
Hanoi, Vietnam
duc.duongminh@hust.edu.vn

Quy-Thinh Dao

School of Electrical and Electronic Engineering
Hanoi University of Science and Technology
Hanoi, Vietnam
thinh.daoquy@hust.edu.vn

Trong-Hieu Do

School of Electrical and Electronic Engineering
Hanoi University of Science and Technology
Hanoi, Vietnam
hieu.dotrong@hust.edu.vn

Received: 5 August 2022 | Revised: 23 August 2022 | Accepted: 24 August 2022

Abstract-The input shaping technique is widely used as feedforward control for vibration suppression of flexible dynamic systems. The main disadvantage of the input shaping technique is the increasing system time response since the input shaper contains time delay parts. However, with the same reference input, the actuator effort in the case of using an input shaper is smaller than the one in the case without an input shaper. Thus, it is possible to decrease the system response time by designing the feedback controller to maximize the actuator effort. This paper proposes a design approach to design the Proportional-Derivative (PD) controller for position control of the actuator so that the settling time of the flexible system with input shaper is minimized. The actuator system with a PD controller is equivalent to a critically damped system, and the condition for the controller gains is established. In addition, the settling time and actuator effort with shaped step input are calculated. The controller gains can be determined by solving the settling time optimization problem with the actuator effort constraint. The effectiveness of the proposed approach is verified via experiments with an overhead crane model.

Keywords-flexible system; input shaping; PD controller; settling time optimization; overhead crane

I. INTRODUCTION

The vibration of flexible dynamic systems such as live load and flexible beam systems [1-3] and flexible robot manipulator and cranes [4-12] often causes a decrease in operation speed and accuracy. Due to sensor noise and unmodeled flexible dynamic problems, vibration suppression control using feedback control has often substantial limitations [4-7]. Open-loop control is effective and widely used for the vibration suppression control of flexible machines. If the vibration dynamics are known with some confidence, then several

techniques for modifying commands can suppress the system's vibration [8-13]. Among them, input shaping [13], which convolves a sequence of impulses with the command signal, is one of the most attractive techniques. Various improvements and applications of input shaping have been reported [14, 15]. The input shaping technique has also been used along with feedback control to optimize the system performance [16-24]. In [16-18], the concurrent design of the Proportional-Derivative (PD) controller and input shaping was considered. The PD controller parameters were chosen to fasten the feedback system response, and the input shaping was designed to eliminate the natural vibration frequency of the PD feedback control system. The same idea was deployed in [19] for the combination of input shaping technique and a Linear Quadratic Regulator (LQR) feedback control system. These works only considered the single mode vibration. The design technique was proposed for a feedback control system with multi-mode vibration in [20-21]. The vibration model uncertainty was also considered when combining input shaping and feedback controller [22-24].

The above mentioned studies used input shaping that eliminates the vibration of the feedback system to optimize the system performance, not to suppress the vibration of a flexible system. In general, the vibration suppression control of a flexible dynamic system includes a feedback control part for actuator position control and a feed-forward control part for vibration control, as shown in Figure 1. When using an Input Shaper (IS) as feed-forward control, the IS only depends on the vibration model, not the feedback system. The feedback control is usually designed independently with the feed-forward controller. This design method is simple but does not optimize the system performance.

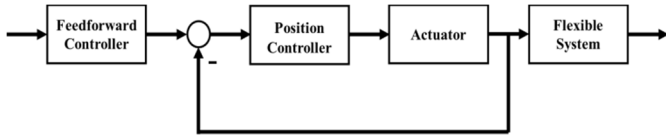


Fig. 1. Feed-forward control structure for vibration suppression control.

Since the IS includes time delay parts that slow down the system, various efforts have been made to shorten the delay, see [14] for more details. However, most of them have not considered combining a feedback controller to reduce the system response. In this paper, a design technique to optimize the time performance of the system with the IS is proposed. At first, the IS is designed using the vibration’s parameters. Next, the PD controller is chosen to minimize settling time while keeping the actuator effort within the acceptable range. For this purpose, design techniques such as the one in [16] can be applied. However, that technique can only be applied to an under-damped feedback system. In many applications, the under-damped system is not expected since the existence of overshoot may cause limit excess. Thus, in this paper, we consider a design technique for a critically damped system. The PD feedback controller is designed to optimize the settling time, in consideration that the IS has been added to shape the input. The actuator effort is used as a design constraint. The settling time and actuator effort calculation are established such that the optimization problem can be easily solved by an optimization toolbox.

II. INPUT SHAPING METHOD

Input preshaping [13] is a feed-forward control technique for vibration suppression. The idea of input preshaping method is to cancel the vibration of an impulse input by generating another impulse that causes the inverse phase vibration with the first one. Let’s consider a simple vibratory system that can be expressed as second order system as following:

$$G_s = \frac{Y(s)}{V(s)} = \frac{\omega_0^2}{s^2 + 2\omega_0\xi_0s + \omega_0^2} \quad (1)$$

where ω_0 is the undamped natural frequency, ξ_0 is the damping ratio of the system, $Y(s)$ and $V(s)$ are the Laplace transforms of output $y(t)$ and input $v(t)$ respectively. If an impulse input with amplitude A_i is put into the system at time t_i , then the output response $y(t)$ is calculated as:

$$y(t) = B_i \cdot \sin(\alpha \cdot t + \phi_i) \quad (2)$$

where $B_i = A_i \cdot \frac{\omega_0}{\sqrt{1-\xi_0^2}} e^{-\xi_0\omega_0(t-t_i)}$, $\alpha = \omega_0\sqrt{1-\xi_0^2}$, and

$$\phi_i = \omega_0\sqrt{1-\xi_0^2}t_i.$$

In order to suppress the vibration caused by the impulse, we consider applying a second impulse to the system. Then the response of two impulses is calculated as:

$$y = B_1 \cdot \sin(\alpha \cdot t + \phi_1) + B_2 \cdot \sin(\alpha \cdot t + \phi_2) \quad (3)$$

Using the trigonometric relation, we can obtain:

$$y = B \cdot \sin(\alpha \cdot t + \phi_{th}) \quad (4)$$

where:

$$\begin{cases} B = \sqrt{(B_1\sin\phi_1 + B_2\sin\phi_2)^2 + (B_1\cos\phi_1 + B_2\cos\phi_2)^2} \\ \phi_{th} = \tan^{-1} \left(\frac{B_1\sin\phi_1 + B_2\sin\phi_2}{B_1\cos\phi_1 + B_2\cos\phi_2} \right) \end{cases}$$

By setting the response of two impulses equal to zero after applying the last impulse, we can easily obtain (supposing that the time of applying the first impulse is $t_1 = 0$ and the impulse amplitude are normalized $A_1 + A_2 = 1$):

$$\begin{bmatrix} A_i \\ t_i \end{bmatrix} = \begin{bmatrix} \frac{1}{1+K} & \frac{K}{1+K} \\ 0 & \Delta t \end{bmatrix} \quad (5)$$

$$\text{where } \begin{cases} K = \frac{-\pi \cdot D}{e^{\sqrt{1-D^2}}} \\ \Delta t = \frac{\pi}{\omega_0 \cdot \sqrt{1-D^2}} \end{cases}$$

The two-impulse shaper is called the Zero Vibration (ZV) shaper. In general, if we apply N impulses with amplitude A_i and at time t_i ($i = 1, \dots, N$), then the response of N impulses is calculated as:

$$y = \sum_{i=1}^N y_i(t) = \sum_{i=1}^N B_i \cdot \sin(\alpha \cdot t + \phi_i) \quad (6)$$

$$\text{where } \begin{cases} B = \sqrt{(\sum_{i=1}^N B_i \sin\phi_i)^2 + (\sum_{i=1}^N B_i \cos\phi_i)^2} \\ \phi_{th} = \tan^{-1} \left(\frac{\sum_{i=1}^N B_i \sin\phi_i}{\sum_{i=1}^N B_i \cos\phi_i} \right) \end{cases}$$

By setting the amplitude and its derivative equal to zero after applying the last impulse, we can obtain the result for 3 impulses ($N=3$) as follows:

$$\begin{bmatrix} A_i \\ t_i \end{bmatrix} = \begin{bmatrix} \frac{1}{(1+K)^2} & \frac{2K}{(1+K)^2} & \frac{K^2}{(1+K)^2} \\ 0 & \Delta t & 2\Delta t \end{bmatrix} \quad (7)$$

The three-impulse shaper or Zero Vibration Derivative (ZVD) shaper is more robust than the ZV shaper. More results can be seen in [14, 15]. By convolving the reference input and the above impulse series, the vibration can be suppressed. This paper will apply vibration suppression control using input preshaping with two and three impulses. It is noted that the response of the system with input preshaping is slower than that without input preshaping. The delay time is Δt with ZV and $2\Delta t$ with ZVD input preshaping.

III. CONTROLLER DESIGN

In a flexible system, the actuator, such as an electrical motor, is controlled by a motor driver under velocity control mode. The actuator then can be modeled as follows:

$$\frac{X(s)}{U(s)} = G_p(s) = \frac{K_c}{(T_c s + 1)s} \quad (8)$$

where K_c is the gain and T_c is time constant of the system, $U(s)$ and $X(s)$ are the Laplace transforms of control voltage input $u(t)$ and actuator position $x(t)$ respectively.

The system structure is shown in Figure 2, where $G_{PD}(s)$ is the transfer function of the feedback controller, $G_p(s)$ is the transfer function of the plant (actuator and driver). The IS includes N impulses designed based on the flexible system’s vibration frequency and damping. We consider the system step

input to design the PD controller for position control. System response and settling time are calculated. In addition, the actuator effort is also determined. Then the settling time optimization with actuator effort constraint can be established, and the selection of PD controller parameters can be made by solving this optimization problem.

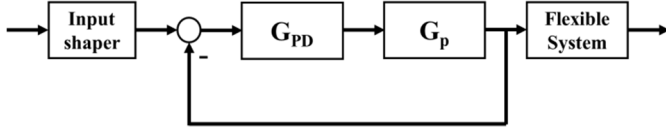


Fig. 2. Input shaper – PD feedback control structure.

A. System Output Response

The PD controller can be described by the following transfer function:

$$G_{PD}(s) = K_D s + K_P \quad (9)$$

where $K_P \geq 0$ is the proportional gain and $K_D \geq 0$ is the derivative gain. Then, the transfer function of the closed-loop system is:

$$G_{CL} = \frac{G_p G_{PD}}{G_p G_{PD} + 1} = \frac{\frac{K_c K_D}{T_c} s + \frac{K_c K_P}{T_c}}{s^2 + \frac{K_c K_P + 1}{T_c} s + \frac{K_c K_P}{T_c}} \quad (10)$$

By setting: $\frac{K_c K_D}{T_c} = M$ and $\frac{K_c K_P}{T_c} = N$ we have:

$$G_{CL} = \frac{Ms + N}{s^2 + \frac{MT_c + 1}{T_c} s + N} = \frac{X(s)}{R(s)} \quad (11)$$

Because the underdamped system is not expected, the denominator of $G_{CL}(s)$ must have negative real roots. In addition, we require minimum response time. Thus, the denominator should have double negative roots. The condition for being double root is:

$$\left(\frac{MT_c + 1}{2T_c}\right)^2 = N \Leftrightarrow \left(\frac{K_c K_D + 1}{2T_c}\right)^2 = \frac{K_c K_P}{T_c} \quad (12)$$

Now, we introduce an input step with magnitude L into the system at time t_0 , $R(s) = \frac{L e^{-t_0 s}}{s}$, the response of the feedback system is:

$$X(s) = \frac{L e^{-t_0 s}}{s} \frac{Ms + N}{s^2 + \frac{MT_c + 1}{T_c} s + N} \quad (13)$$

Thus, the response of the system with single step input can be expressed as:

$$x(t) = \frac{L.M}{a^2} \left[\alpha - \alpha e^{-a(t-t_0)} + a(a - \alpha)(t - t_0) e^{-a(t-t_0)} \right] \quad (14)$$

where $a = \frac{M.T_c + 1}{2T_c}$ and $\alpha = \frac{N}{M}$.

Since the overshoot is not expected to appear, $x(t)$ must be a non-decreasing or non-increasing function in the region $t \geq t_0$. Thus, the root t_r of equation $\dot{x}(t) = 0$ must be outside the region $t \geq t_0$, or $t_r < t_0$. Solving the equation $\dot{x}(t) = 0$ we obtain $t_r = t_0 + \frac{a}{a - \alpha}$. Thus:

$$t_r < t_0 \Leftrightarrow \frac{a}{a - \alpha} < 0 \Leftrightarrow a < \alpha \Leftrightarrow \frac{K_D^2}{T_c} < K_P \quad (15)$$

From the system response with single step input (14), the response of the system with convolved step command after step k is:

$$y(t) = \frac{LM}{a^2} \left[\alpha \sum_{j=1}^k L_i - \alpha \sum_{j=1}^k L_i e^{-a(t-t_j)} + a(a - \alpha) \sum_{j=1}^k L_i (t - t_j) e^{-a(t-t_j)} \right] \quad (16)$$

Since $\frac{M}{a^2} \alpha = 1$, the response $y(t)$ can be rewritten as:

$$y(t) = L \sum_{j=1}^k L_j - L \sum_{j=1}^k L_j e^{-a(t-t_j)} + L(M - a) \sum_{j=1}^k L_j (t - t_j) e^{-a(t-t_j)} \quad (17)$$

B. Settling Time

Settling time is a primary concern for most industrial applications. The faster the settling time, the higher throughput and accuracy are. The system is defined to be settled when the output response falls below a certain percentage (usually 5% or 2%) of the step magnitude. The settling time is the required time for the output curve to reach and stay within a range of a certain percentage (usually 5% or 2%) of the final value. In this paper, we use the range of 5% to calculate settling time. We can describe the definition of settling time t_s as the following conditions:

$$1 - \frac{y(t)}{L} \leq 0.05, \forall t \geq t_s \quad (18)$$

$$1 - \frac{y(t_s)}{L} = 0.05 \quad (19)$$

It is obvious that settling time is determined after the final step. Thus, the output $y(t)$ to calculate settling time is the output with N steps. Since $\sum_{j=1}^N L_j = 1$, and substituting (17) into (19), we have:

$$1 - \frac{y(t_s)}{L} = \sum_{j=1}^N L_j e^{-a(t_s-t_j)} - (M - a) \sum_{j=1}^N L_j (t_s - t_j) e^{-a(t_s-t_j)} = 0.05 \quad (20a)$$

Moreover, since $t_s > t_n$, it can make the approximation $e^{-a(t_s-t_j)} \cong 0$ and $(t_s - t_j) e^{-a(t_s-t_j)} \cong 0$ with $j < N$. Then (20a) becomes:

$$L_n [e^{-a(t_s-t_n)} - (M - a)(t_s - t_n) e^{-a(t_s-t_n)}] = 0.05 \quad (20b)$$

Using the Lambert W function $W(z)$ (i.e. $z = W(z) e^{W(z)}$) [25], the settling time t_s can be determined as:

$$t_s = t_n + \frac{1}{M - a} - \frac{1}{a} W\left(\frac{0.05 a e^{\frac{M - a}{a}}}{a(M - a)}\right) \quad (21)$$

C. Actuator Effort

With reference input as step input, we are also interested in the actuator effort when designing the controller. According to Figure 2, with the input $R(s)$, the actuator effort can be determined as:

$$U(s) = \frac{G_{PD}}{G_{PD} \cdot G_p + 1} \cdot R(s) = \frac{s(T_c s + 1)(K_c K_D s + K_c K_P)}{T_c s^2 + (K_c K_D + 1)s + K_c K_P} \cdot R(s) \quad (22)$$

If the input $r(t)$ is the step input with magnitude L at the time t_0 , $R(s) = \frac{Le^{-t_0s}}{s}$, then:

$$U(s) = Le^{-t_0s} \frac{(T_c s + 1)(K_c K_D s + K_c K_P)}{T_c s^2 + (K_c K_D + 1)s + K_c K_P} \quad (23)$$

The actuator effort can be calculated as:

$$u(t) = L \frac{K_P T_c - K_c K_D^2}{T_c} [e^{-a(t-t_0)} + (\alpha_1 - a)(t - t_0)e^{-a(t-t_0)}] \quad (24)$$

where $\alpha_1 = \frac{K_P - K_c K_P K_D}{T_c K_P - K_c K_D^2}$. Then, the actuator effort with convolved step command after step k is:

$$u(t) = \frac{K_P T_c - K_c K_D^2}{T_c} \times \sum_{j=1}^k L_j [e^{-a(t-t_j)} + (\alpha_1 - a)(t - t_j)e^{-a(t-t_j)}] \quad (25)$$

The actuator effort $u(t)$ can be represented as the form:

$$u(t) = P_k e^{-at} + Q_k t e^{-at} \quad (26)$$

where:

$$P_k = \frac{K_P T_c - K_c K_D^2}{T_c} \sum_{j=1}^k L_j [1 - (\alpha_1 - a)t_j] e^{at_j}$$

$$Q_k = \frac{K_P T_c - K_c K_D^2}{T_c} \sum_{j=1}^k L_j (\alpha_1 - a) e^{at_j}$$

To find the maximum value of $u(t)$, we solve the equation:

$$\dot{u}(t) = [(-aP_k + Q_k) - aQ_k t] e^{-at} = 0 \quad (27)$$

Thus, the maximum value of $u(t)$ can be obtained at time:

$$t_{ku} = \frac{Q_k - aP_k}{aQ_k} \quad (28)$$

It is noted that we can only consider $u(t)$ after step k , and $u(t)$ is decreased when $t > t_{ku}$. Therefore, the maximum value of actuator effort U_{kmax} is calculated as:

$$U_{kmax} = \begin{cases} P_k e^{-at_k} + Q_k t_k e^{-at_k} & \text{if } t_{ku} \leq t_k \\ P_k e^{-at_{ku}} + Q_k t_{ku} e^{-at_{ku}} & \text{if } t_{ku} > t_k \end{cases} \quad (29)$$

To guarantee that $u(t)$ is within the allowable actuator effort range, the following constraint is required after the step corresponding to each impulse:

$$U_{kmax} \leq U_{max} \text{ for all } k = 1, \dots, N \quad (30)$$

where U_{max} is the maximum allowable actuator effort.

D. Controller Designing

The designing process of actuator position control using a PD controller and vibration suppression control using input shaping for a flexible dynamic system is:

Step 1: Determine the system vibration parameters, including natural vibration frequency and damping factor.

Step 2: Choose the appropriate input preshaping techniques such as ZV, ZVD, etc. See [14, 15] for more details about IS techniques.

Step 3: Choose the PD controller parameters K_P and K_D to minimize the system settling time by solving the following

optimization problem: minimizing (21) with constraints (12), (15), and (30).

IV. APPLICATION TO OVERHEAD CRANE

Figure 3 describes the overhead crane. In this figure, x is the cart's position, l is the rope length, m is the load mass, M is the cart mass, and θ is the angle between the rope and the vertical axis (Y axis). According to [26], the overhead crane linearized model can be described as:

$$F_x = (M + m)\ddot{x} + b_x \dot{x} + ml\ddot{\theta} \quad (31)$$

$$-\ddot{x} = l\ddot{\theta} + b_\theta \dot{\theta} + g\theta \quad (32)$$

where b_x and b_θ are the equivalent viscous damping of the cart and the load respectively. It can be seen that (31) describes the relation between the input force and the cart's position. The load angle plays the role of disturbance. Equation (32) describes the effect of the cart's motion to the vibration of the load.

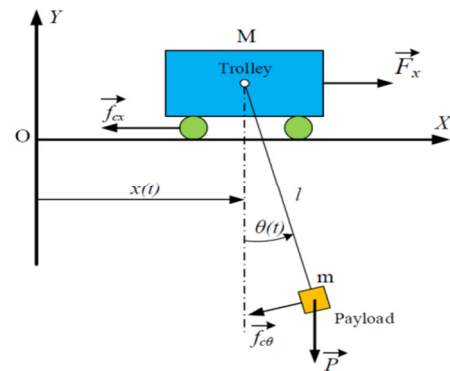


Fig. 3. Overhead crane model.

In practice, the cart is controlled by a motor with a driver. That can allow us to control the velocity of the cart. Therefore, to control the cart's position, we use the motor model with a driver instead of (31). The cart plays the role of an actuator in a flexible system and has (8) as the transfer function. The control of the overhead crane is to move the load to the desired position while suppressing the load vibration. To control the cart's position precisely, a PD controller is used. In addition, to suppress the load vibration, input preshaping is applied.

The actual experiments are conducted with the overhead crane model shown in Figure 4. The vibration model can be calculated from (32), however, the model's parameters may not be precise. Thus, we measured the sway angle and identified the natural vibration frequency and damping factor. The experiment parameters are shown in Table I.

TABLE I. EXPERIMENT PARAMETERS

Parameter	Values
K_c	4
T_c	0.2
ω_0	4.45 rad/s
ξ_0	0.007
g	9.81 m/s ²
U_{max}	10 V

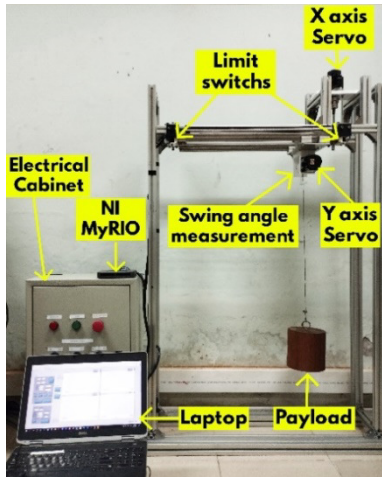


Fig. 4. Experimental crane system.

Then, two types of input shaping including ZV and ZVD can be designed using (5) for ZV and (7) for ZVD. Using the designed ISs, the PD controllers that optimize the settling time were calculated. We call them optimized PD-ZV and optimized PD-ZVD. In addition, the PD controller that optimizes the settling time of the feedback system using step input only and with the same constraint is also calculated. We call it optimized PD without IS. The ISs (5) and (7) are then applied to the optimized PD without IS. We call them ZV-optimized PD and ZVD-optimized PD without IS. The results are shown in Table II.

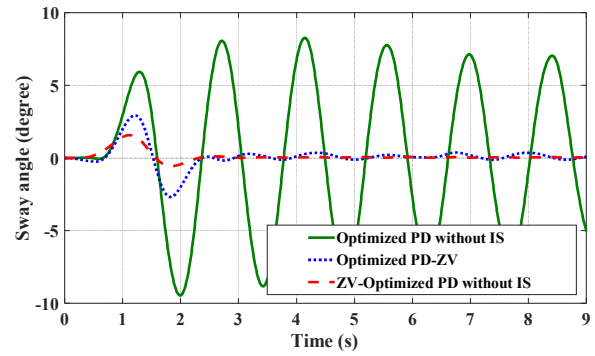


Fig. 7. Sway angle in three cases: optimized PD without IS, ZV-optimized PD without IS, and optimized PD-ZV.

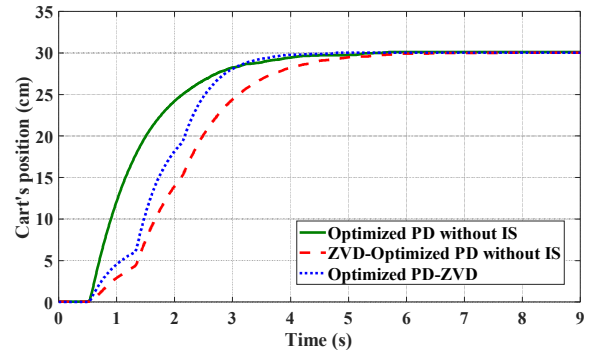


Fig. 8. Cart's position in three cases: optimized PD without IS, ZVD-optimized PD without IS, and optimized PD-ZVD.

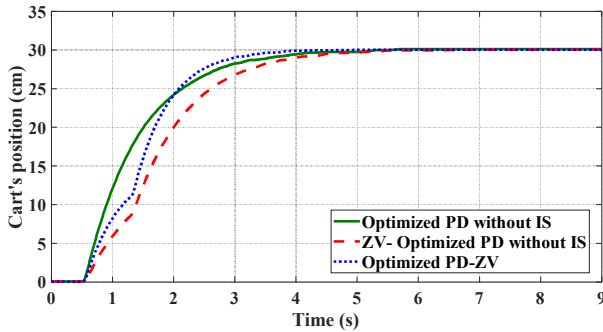


Fig. 5. Cart's position in three cases: optimized PD without IS, ZV-optimized PD without IS, and optimized PD-ZV.

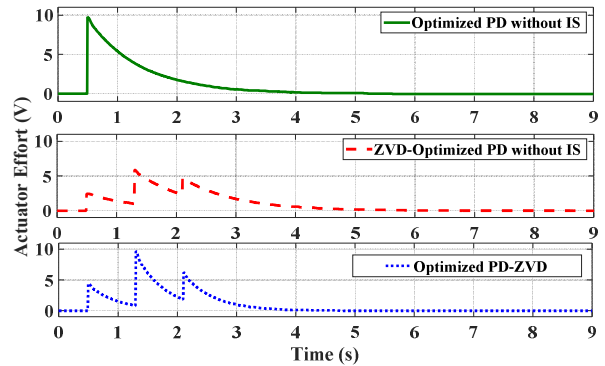


Fig. 9. Actuator effort in three cases: optimized PD without IS, ZVD-optimized PD without IS, and optimized PD-ZVD.

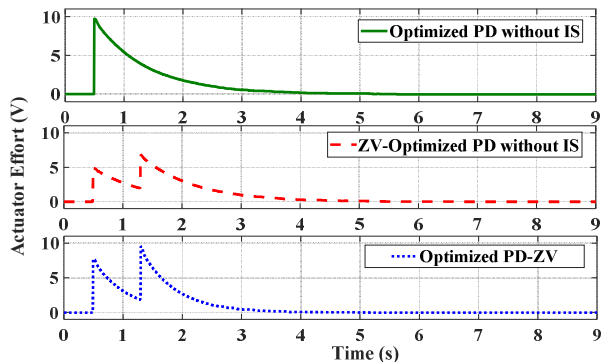


Fig. 6. Actuator effort in three cases: optimized PD without IS, ZV-optimized PD without IS, and optimized PD-ZV.

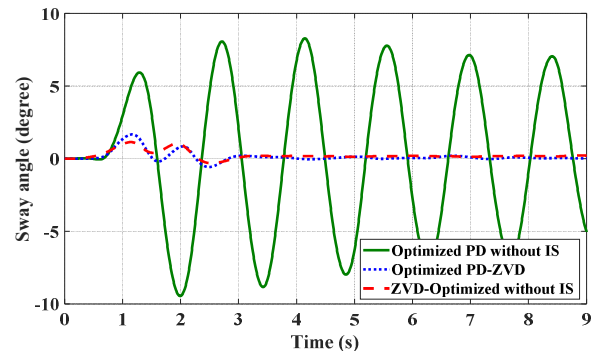


Fig. 10. Sway angle in three cases: optimized PD without IS, ZVD-optimized PD without IS, and optimized PD-ZVD.

TABLE II. CONTROLLER PARAMETERS AND SETTLING TIME

Parameter	Values		
	Optimized PD without IS	Optimized PD-ZV	Optimized PD-ZVD
K_p	0.325	0.52	0.59
K_d	0.01	0.07	0.09
Settling time (s)	2.66	2.27	2.64
	Using ZV: 3.18 Using ZVD: 3.67		

The experimental results are shown in Figure 5-9. It is clear that ZV and ZVD can suppress the payload vibration significantly. In the case of optimized PD without IS, the settling time is 2.66s. But when the IS is applied to the vibration suppression control, the settling time increases to 3.18s for ZV shaper and 3.67s for ZVD shaper. In addition, the actuator effort also reduces from 10V in the case of optimized PD without IS to 6.80V and 5.90V when applying ZV and ZVD shapers respectively. Therefore, we should design the PD controller in consideration of using IS at the system input. As a result, the actuator effort is larger but still in the required limit, and the system moves faster with settling time only 2.27s for ZV and 2.64s for ZVD shapers.

It is also found that in the case of optimized PD-ZV the settling time is smaller than the one in the case of ZV-optimized PD without IS, but the residual vibration magnitude is larger. The reason for this is the difference between the actual vibration frequency and the designed vibration frequency and the effect of the feedback system to the response of the IS shaper. This can be improved by using ZVD shaper. It is clear that in the case of optimized PD-ZVD the settling time is smaller than the one in the case of ZVD-optimized PD without IS, and the residual vibration magnitude is almost the same.

V. CONCLUSIONS

The current paper proposes a design process for the PD controller of the actuator in a flexible system that uses input shaper for vibration suppression control. The controller gains are chosen such that the feedback system is of the critically damped type and system's settling time is minimized while keeping the actuator effort constraint. The experiments with overhead crane model show the effectiveness of the proposed designing process. The settling time is reduced, in comparison to the case of the optimizing PD controller without considering the use of the input shaper. In the future, a designing tool will be developed to apply the proposed designing process for a real flexible system. In addition, the designing process for the system with time varying vibration frequency is also considered.

ACKNOWLEDGMENT

The paper is supported by the Hanoi University of Science and Technology project T2021-PC-002.

REFERENCES

[1] I. Esen and M. A. Koç, "Dynamic response of a 120 mm smoothbore tank barrel during horizontal and inclined firing positions," *Latin American Journal of Solids and Structures*, vol. 12, pp. 1462–1486, Aug. 2015, <https://doi.org/10.1590/1679-78251576>.

[2] I. Esen, "Dynamic response of a functionally graded Timoshenko beam on two-parameter elastic foundations due to a variable velocity moving mass," *International Journal of Mechanical Sciences*, vol. 153–154, pp. 21–35, Apr. 2019, <https://doi.org/10.1016/j.ijmecs.2019.01.033>.

[3] I. Esen, "Dynamic response of functional graded Timoshenko beams in a thermal environment subjected to an accelerating load," *European Journal of Mechanics - A/Solids*, vol. 78, Nov. 2019, Art. no. 103841, <https://doi.org/10.1016/j.euromechsol.2019.103841>.

[4] M. Balas, "Feedback control of flexible systems," *IEEE Transactions on Automatic Control*, vol. 23, no. 4, pp. 673–679, Aug. 1978, <https://doi.org/10.1109/TAC.1978.1101798>.

[5] D. Antic, Z. Jovanovic, S. Peric, S. Nikolic, M. Milojkovic, and M. Milosevic, "Anti-Swing Fuzzy Controller Applied in a 3D Crane System," *Engineering, Technology & Applied Science Research*, vol. 2, no. 2, pp. 196–200, Apr. 2012, <https://doi.org/10.48084/etasr.146>.

[6] C. T. Kiang, A. Spowage, and C. K. Yoong, "Review of Control and Sensor System of Flexible Manipulator," *Journal of Intelligent & Robotic Systems*, vol. 77, no. 1, pp. 187–213, Jan. 2015, <https://doi.org/10.1007/s10846-014-0071-4>.

[7] K. G. Aktas and I. Esen, "State-Space Modeling and Active Vibration Control of Smart Flexible Cantilever Beam with the Use of Finite Element Method," *Engineering, Technology & Applied Science Research*, vol. 10, no. 6, pp. 6549–6556, Dec. 2020, <https://doi.org/10.48084/etasr.3949>.

[8] L. Cui, H. Wang, and W. Chen, "Trajectory planning of a spatial flexible manipulator for vibration suppression," *Robotics and Autonomous Systems*, vol. 123, Jan. 2020, Art. no. 103316, <https://doi.org/10.1016/j.robot.2019.103316>.

[9] D. Lee and C.-W. Ha, "Optimization Process for Polynomial Motion Profiles to Achieve Fast Movement With Low Vibration," *IEEE Transactions on Control Systems Technology*, vol. 28, no. 5, pp. 1892–1901, Sep. 2020, <https://doi.org/10.1109/TCST.2020.2998094>.

[10] H. Karagülle, L. Malgaca, M. Dirilmiş, M. Akdağ, and Ş. Yavuz, "Vibration control of a two-link flexible manipulator," *Journal of Vibration and Control*, vol. 23, no. 12, pp. 2023–2034, Jul. 2017, <https://doi.org/10.1177/1077546315607694>.

[11] H. J. Yoon, S. Y. Chung, H. S. Kang, and M. J. Hwang, "Trapezoidal Motion Profile to Suppress Residual Vibration of Flexible Object Moved by Robot," *Electronics*, vol. 8, no. 1, Jan. 2019, Art. no. 30, <https://doi.org/10.3390/electronics8010030>.

[12] B. Spruogis, A. Jakstas, V. Gican, V. Turla, and V. Moksins, "Further Research on an Anti-Swing Control System for Overhead Cranes," *Engineering, Technology & Applied Science Research*, vol. 8, no. 1, pp. 2598–2603, Feb. 2018, <https://doi.org/10.48084/etasr.1774>.

[13] N. C. Singer and W. P. Seering, "Preshaping Command Inputs to Reduce System Vibration," *Journal of Dynamic Systems, Measurement, and Control*, vol. 112, no. 1, pp. 76–82, Mar. 1990, <https://doi.org/10.1115/1.2894142>.

[14] W. Singhose, "Command shaping for flexible systems: A review of the first 50 years," *International Journal of Precision Engineering and Manufacturing*, vol. 10, no. 4, pp. 153–168, Oct. 2009, <https://doi.org/10.1007/s12541-009-0084-2>.

[15] C.-G. Kang, "Impulse Vectors for Input-Shaping Control: A Mathematical Tool to Design and Analyze Input Shapers," *IEEE Control Systems Magazine*, vol. 39, no. 4, pp. 40–55, Dec. 2019, <https://doi.org/10.1109/MCS.2019.2913610>.

[16] M. Kenison and W. Singhose, "Concurrent Design of Input Shaping and Proportional Plus Derivative Feedback Control," *Journal of Dynamic Systems, Measurement, and Control*, vol. 124, no. 3, pp. 398–405, Jul. 2002, <https://doi.org/10.1115/1.1486009>.

[17] J. R. Huey, "The Intelligent Combination of Input Shaping and PID Feedback Control," Ph.D. dissertation, Georgia Institute of Technology, Atlanta, GA, USA, 2006.

[18] J. R. Huey and W. Singhose, "Design of proportional-derivative feedback and input shaping for control of inertia plants," *IET Control Theory & Applications*, vol. 6, no. 3, pp. 357–364, Feb. 2012, <https://doi.org/10.1049/iet-cta.2010.0456>.

- [19] M. Muenchhof and T. Singh, "Concurrent Feed-forward/Feed-back Design for Flexible Structures," in *AIAA Guidance, Navigation, and Control Conference and Exhibit*, Monterey, CA, USA, Aug. 2002, <https://doi.org/10.2514/6.2002-4941>.
- [20] R. Mar, A. Goyal, V. Nguyen, T. Yang, and W. Singhose, "Combined input shaping and feedback control for double-pendulum systems," *Mechanical Systems and Signal Processing*, vol. 85, pp. 267–277, Feb. 2017, <https://doi.org/10.1016/j.ymssp.2016.08.012>.
- [21] D. Newman and J. Vaughan, "Concurrent Design of Linear Control with Input Shaping for a Two-Link Flexible Manipulator Arm," *IFAC-PapersOnLine*, vol. 51, no. 14, pp. 66–71, Jan. 2018, <https://doi.org/10.1016/j.ifacol.2018.07.200>.
- [22] M.-C. Pai, "Closed-loop input shaping control of vibration in flexible structures using discrete-time sliding mode," *International Journal of Robust and Nonlinear Control*, vol. 21, no. 7, pp. 725–737, 2011, <https://doi.org/10.1002/rnc.1618>.
- [23] M.-C. Pai, "Closed-Loop Input Shaping Control of Vibration in Flexible Structures via Adaptive Sliding Mode Control," *Shock and Vibration*, vol. 19, no. 2, pp. 221–233, 2012, <https://doi.org/10.3233/SAV-2011-0625>.
- [24] J. Oliveira, P. M. Oliveira, T. M. Pinho, and J. B. Cunha, "PID Posicast Control for Uncertain Oscillatory Systems: A Practical Experiment," *IFAC-PapersOnLine*, vol. 51, no. 4, pp. 416–421, Jan. 2018, <https://doi.org/10.1016/j.ifacol.2018.06.130>.
- [25] R. M. Corless, G. H. Gonnet, D. E. G. Hare, D. J. Jeffrey, and D. E. Knuth, "On the LambertW function," *Advances in Computational Mathematics*, vol. 5, no. 1, pp. 329–359, Dec. 1996, <https://doi.org/10.1007/BF02124750>.
- [26] D. Qian and J. Yi, *Hierarchical Sliding Mode Control for Under-actuated Cranes*. Berlin, Heidelberg: Springer, 2015.